Electronic excitation and oscillator strength of ethyl bromide by vacuum ultraviolet photoabsorption and electron energy loss spectroscopy

A. Giuliani, F. Motte-Tollet, J. Delwiche, N. J. Mason, N. C. Jones, J. M. Gingell, I. C. Walker, and M.-J. Hubin-Franskin

Citation: The Journal of Chemical Physics **112**, 6285 (2000); doi: 10.1063/1.481273
View online: http://dx.doi.org/10.1063/1.481273
View Table of Contents: http://scitation.aip.org/content/aip/journal/jcp/112/14?ver=pdfcov
Published by the AIP Publishing

Electronic excitation and oscillator strength of ethyl bromide by vacuum ultraviolet photoabsorption and electron energy loss spectroscopy

A. Giuliani and F. Motte-Tollet
Laboratoire de Spectroscopie d'Electrons Diffusés, Université de Liège, Institut de Chimie-Bât. B6c, B-4000 Liège, Belgium

J. Delwiche
Thermodynamique et Spectroscopie, Université de Liège, Institut de Chimie-Bât. B6c, B-4000 Liège, Belgium

N. J. Mason and N. C. Jones
Department of Physics and Astronomy, University College London, Gower Street, London WC1E 6BT, United Kingdom

J. M. Gingell
Department of Chemistry, Christopher Ingold Laboratories, 20 Gordon Street, London WC1H OAJ, United Kingdom

I. C. Walker
Department of Chemistry, Heriot-Watt University, Riccarton, Edinburgh EH14 4AS, United Kingdom

M.-J. Hubin-Franskin[a)]
Laboratoire de Spectroscopic d'Electrons Diffusés, Université de Liège, Institut de Chimie-Bât. B6c, B-4000 Liège, Belgium

(Received 2 December 1999; accepted 20 January 2000)

The high resolution vacuum ultraviolet photoabsorption spectrum of ethyl bromide has been recorded between 5 and 10.15 eV (248–122 nm) using synchrotron radiation. It exhibits a broad structureless valence band centred at 6.1 eV of low cross section followed by a region dominated by excitation of Rydberg states. A high resolution photoelectron spectrum (PES) of the lowest energy ionization band has been obtained and provides ionization energies necessary for identification of related Rydberg-excited states. Also, analysis of the vibrational fine structure in the PES has allowed identification of the normal vibrational modes excited and their wave numbers in the ion. These data, in turn, have been used in the assignment of the lowest energy photoabsorption bands arising from electron excitation into the 5*s* Rydberg orbital. The electron energy loss spectrum, recorded from 6.5 to 14.1 eV, under electric-dipole conditions, confirms the magnitude of the photoabsorption cross-section values obtained using the synchrotron radiation and extends the differential and optical oscillator strength values up to 14.004 eV. © *2000 American Institute of Physics.* [S0021-9606(00)01814-6]

I. INTRODUCTION

During the last two decades, the electronically excited states of the alkyl bromides have attracted increasing interest. A vacuum ultraviolet (VUV) photoabsorption spectrum of such a molecule shows a weak broadband at low excitation energy, labeled the *A* band, due to a transition of the type $4p(\mathrm{Br}) \rightarrow \sigma^*(\mathrm{C-Br})$. The resulting electronic state is dissociative along the C–Br bond. At higher energy, one finds much more intense and narrow absorption features, traditionally labeled *B*, *C*, *D*,... and attributed to transitions to Rydberg states. Background absorptions underlying some Rydberg bands have been reported[1] and related to excitation of higher valence excited states of σ^* character. Consequently, alkyl bromides are model systems for photodissociation dynamic studies.[2] They may be implicated in some ozone depletion processes when photolyzed in the atmosphere[3,4] and they find applications in surfaces etchant plasmas.[5,6]

Electronic excitation spectra[7–9] and theoretical predictions[10] for the alkyl bromides were first reported in the 1930s. Subsequently, the photoabsorption spectra and extinction coefficients of ethyl bromide have been measured in the region of the valence *A* band and of the lowest energy Rydberg features, for both gas and condensed phases.[11] Around the ionization thresholds (10–10.65 eV), the value of the absorption cross section is modulated by electron promotion into Rydberg orbitals with large quantum numbers. Between 10.65 and 10.8 eV, the cross section is nearly constant (62 Mb) before increasing steeply up to at least 11.8 eV.[12] The oscillator strength of the *A* band measured in different organic solvents and computed by linear combination of atomic orbitals calculations[13] is low. A review of the spectra and assignations has been made and the term values of the *B*, *C*, and *D* bands calculated.[1] The photoabsorption spectrum in

[a)]Directeur de recherche F.N.R.S. Electronic mail: mjfranskin@ulg.ac.be

the 6.59–7.7 eV region has been reexamined and interpreted, by comparison with that of methyl bromide, in terms of electronic origins of the bands *B* and *C*, and accompanying vibrational excitations.[14] Recently, doubling present in the *C* band has been explained by invoking a vibronic coupling between Rydberg states.[15]

We report in this paper new data on the electronic spectroscopy and excitation cross sections of ethyl bromide at 5–14.1 eV. We have made use of VUV photoabsorption with a synchrotron radiation source to provide absolute excitation cross sections and of electron energy loss spectroscopy (EELS) in dipolar excitation conditions to obtain relative cross sections at higher excitation energies. HeI photoelectron spectroscopy (PES) of the highest occupied molecular orbital (HOMO) region, reported at high resolution for the first time, provides the first two ionization energies and the frequencies of normal vibration modes of the molecular ion. These data have been used in the assignment of the vibrational fine structure in the lowest energy Rydberg bands. Optical oscillator strength values derived from the two experimental techniques are reported in the 5.056–14.004 eV region.

II. EXPERIMENTAL METHODS

A. Photoelectron spectroscopy

The photoelectron spectrometer used in these measurements is described in detail elsewhere.[16,17] Briefly, it is fitted with a 180° hemispherical electrostatic analyzer, working in the constant pass-energy mode. The HeI photons (58.4 nm) are produced through a dc discharge in helium in a two-stage differentially pumped lamp. The spectrum was recorded by sweeping the retarding voltage between the chamber and the entrance slit of the analyzer in 2 meV steps and was corrected for the transmission of the analyzing system. The resolution was about 25 meV and the ionization energy scale was calibrated using the xenon peaks ($^2P_{3/2}$: 12.123 eV and $^2P_{1/2}$: 13.436 eV[18]). The raw spectrum was deconvoluted in order to resolve more clearly some features appearing as shoulders and to provide them with more precise energy values. The deconvolution procedure was the Van Cittert method[19] and Allen and Grimm's algorithm.[20] The $Xe^+\ ^2P_{3/2}$ peak was assumed to mimic the instrumental profile.

B. Optical absorption

The VUV photoabsorption spectrum was recorded at the synchrotron radiation source of Daresbury (UK) using the Daresbury Laboratory Molecular Science Absorption Apparatus coupled to beam line 3.1.[21,22] Synchrotron radiation, dispersed by a Seya–Namioka monochromator, enters the absorption cell through a LiF window. The absorption cell is composed of a six-way cross system upon which are fitted: the sample inlet, an outlet coupled to a turbomolecular pump, a Baratron pressure gauge, and the entrance and exit windows for the synchrotron light. The radiation leaves the cell through a LiF window. The spectral range extended from 5 eV (248 nm) to 10.15 eV (122 nm) and was covered by series of 25 nm sections each scanned with 0.05 nm steps. At each wavelength, the transmitted radiation, I_t, was recorded, as well as the sample pressure and the electron beam current of the storage ring. The cell was then emptied and I_0, the radiation intensity through the empty cell, was recorded in the same conditions. I_t and I_0 were normalized to unitary beam current.

The absolute photoabsorption cross section σ_{pa} was obtained by using the Beer–Lambert law:

$$I_t = I_0 \exp(-\sigma_{pa} N x),$$

where N is the target gas number density and x is the path length.

C. Electron energy loss spectroscopy (EELS)

The instrument used (VG-SEELS 400) has been described in detail elsewhere.[23–25] An electrostatic electron energy monochromator fitted with a three-element lens produces a collimated electron beam, defines a narrow energy spread about the mean energy, and focuses the electrons into the collision region. The electron beam intersects the gas beam which flows through an hypodermic needle at 90°. The analyzer system is of the same type as the monochromator. Both electron energy selectors work in the constant pass-energy mode. The signal is detected by an electron multiplier of the continuous dynode type. The electron energy loss spectrum was recorded between 6.5 and 14.1 eV with steps of 8 meV and a resolution of about 36 meV. The operating pressure was 1.5×10^{-5} mbar. The apparatus was used with high incident energy electrons (100 eV) and at a small scattering angle ($\theta\approx0°$), such that dipole (e,e) conditions apply and the energy loss spectrum is comparable to the photoabsorption spectrum. The inelastic scattered intensity was converted to a relative differential oscillator strength distribution, df/dE, using the method of Huebner *et al.*[26]:

$$\frac{df}{dE} \propto \frac{E}{R}\hat{\theta}\left\{\ln\left[1+\left(\frac{\hat{\theta}}{\gamma}\right)^2\right]\right\}^{-1} I(E),$$

where $\gamma=(E/2T)^2(1-E/T)^{-1}$, T is the incident energy, E is the electron energy loss, $I(E)$ is the scattered intensity, $\hat{\theta}$ is the spectrometer angular acceptance ($1.25°\pm0.25$ in this work), and R is one Rydberg.

To obtain absolute values, the EELS data were normalized to the cross section measured at 6.8 eV in the optical experiment. Then, the cross section is calculated from

$$\sigma_{pa} = 109.75\frac{df}{dE},$$

where σ_{pa} is in Mbarn and df/dE is in electron volt^{-1}.

The comparison of the electron impact cross-section values with those of the UV photoabsorption spectrum provides a test for any systematic error in the optical values arising from the line saturation effect and second-order light from the light source and beam line. These effects were found to be negligible in this work.

D. The sample

The sample provided by Aldrich Chemical Ltd. has a purity of 99%. No further purification was undertaken, except for repeated pump–thaw cycles.

TABLE I. Symmetry, wave number, energy, and description of the normal vibrational modes of ethyl bromine in its electronic ground state (Refs. 27,28). N. O. means nonobserved.

Assignation	Wave number (cm^{-1})	Energy (eV)	Description
$\nu_1(a')$	2990.9	0.371	CH_3 antisymmetric stretch
$\nu_2(a')$	2936.7	0.364	CH_2 symmetric stretch
$\nu_3(a')$	2880.0	0.357	CH_3 symmetric stretch
$\nu_4(a')$	1456	0.181	CH_3 antisymmetric deformation
$\nu_5(a')$	1450.7	0.180	CH_2 scissors
$\nu_6(a')$	1385.2	0.172	CH_3 symmetric deformation
$\nu_7(a')$	1257.9	0.156	CH_2 wag
$\nu_8(a')$	1061	0.132	CH_3 in-plane rock
$\nu_9(a')$	964.3	0.120	C–C stretch
$\nu_{10}(a')$	574.9	0.071	C–Br stretch
$\nu_{11}(a')$	294	0.036	C–Br bend
$\nu_{12}(a'')$	3023.7	0.375	CH_2 antisymmetric stretch
$\nu_{13}(a'')$	2990.9	0.371	CH_3 antisymmetric stretch
$\nu_{14}(a'')$	1446	0.179	CH_3 antisymmetric deformation
$\nu_{15}(a'')$	1240	0.154	CH_2 twist
$\nu_{16}(a'')$	1009	0.125	CH_3 out-of-plane rock
$\nu_{17}(a'')$	769.7	0.095	CH_2 rock
$\nu_{18}(a'')$		N.O.	CH_3 torsion

III. RESULTS AND DISCUSSION

Ethyl bromide belongs to the C_s point group and has 18 normal vibrational modes all active in IR and in Raman spectroscopy; wave numbers, energies, symmetries, and descriptions are given in Table I.[27,28] It is a strong $\Omega_c\omega$ spin–orbit coupling case. As previously done successfully for ethyl iodide,[29] we discuss the results using the approximate C_{3v} symmetry, which is that of the precursor CH_3Br. That is, the influence of the methyl group on the spectroscopy of the ion and of the Rydberg states is neglected.

A. The HeI photoelectron spectrum

The region of the photoelectron spectrum investigated here extends from 10.20 to 11 eV [Fig. 1(a)]. It corresponds to ionization of the bromine lone pair.[30,31] In the C_{3v} approximate symmetry, this photoejection leaves the cation in a ^2E state split into $^2E_{3/2}$ and $^2E_{1/2}$ by the spin–orbit coupling.[32] The spectrum shows two intense bands due to the 0–0 transitions to the two ^2E states, in agreement with previous work.[32] In addition it exhibits less intense bands, some of them partly resolved [Fig. 1(b)], observed for the first time and assigned to the vibrational excitation of the ion.

This spectrum is similar to that of methyl bromide,[33] with respect to the energy, the nature, and the relative intensity distribution of the normal vibrational modes excited, showing the assumption of C_{3v} symmetry to be reasonable. From these considerations, the vibrational analysis has been carried out excluding those normal modes involving mostly the methyl group, namely modes ν_1, ν_3, ν_4, ν_6, ν_8, ν_{13}, ν_{14}, ν_{16}, and ν_{18} (see Table I[27,28]).

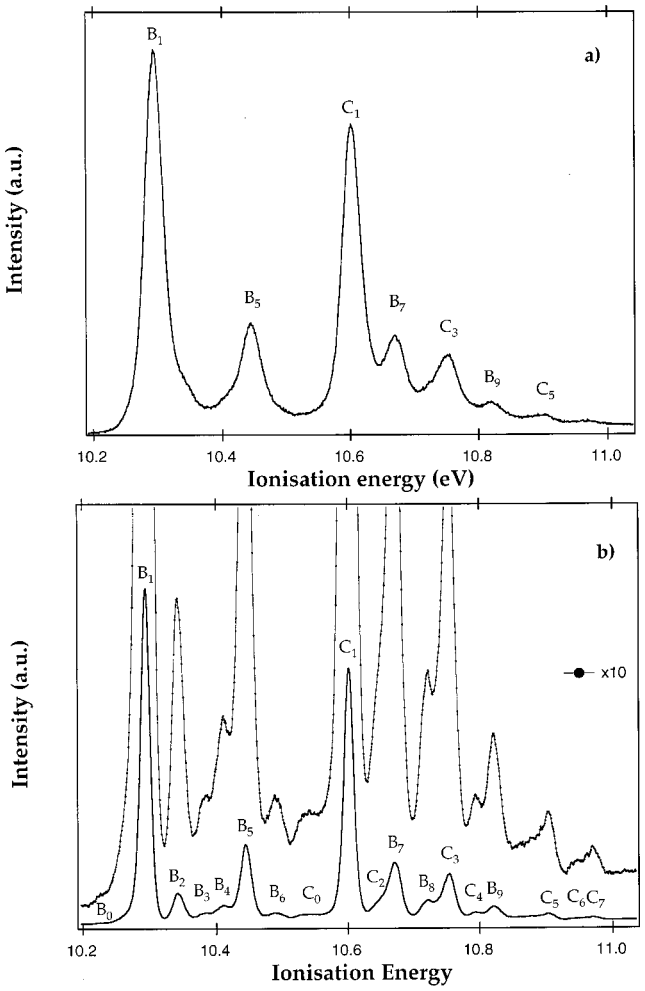

FIG. 1. High resolution HeI photoelectron spectrum of bromoethane corresponding to the HOMO region. (a) Raw photoelectron spectrum. (b) Deconvoluted spectrum with peak label and enlargements in dotted line.

The 0–0 transitions to the $^2E_{3/2}$ and $^2E_{1/2}$ states are attributed to the most intense peaks, B_1 and C_1 at 10.294 eV $\pm$0.005 eV and 10.602 eV$\pm$0.005 eV, respectively, giving a splitting of 0.308 eV$\pm$0.010 eV. These values are in excellent agreement with the literature data.[12,30–32,34]

1. The $^2E_{3/2}$ state and its vibrational progression

A very weak feature B_0, only partly resolved [Fig. 1(b)], is located at 0.068 eV below the electronic origin (B_1) (Table II). It is attributed to a hotband with excitation of $1\nu_{10}$ (C–Br stretch); this assignment follows from its low intensity and its energy value which is close to that of $1\nu_{10}$ in the neutral molecular ground state (0.071 eV, see Table I[27,28]). Feature B_2, appearing as a shoulder in the raw spectrum [Fig. 1(a)] but well resolved after deconvolution [Fig. 1(b)], is assigned to excitation of $1\nu_{10}$, this being also observed in the PES of the HOMO of C_3H_7Br.[34] The most intense vibrational peak accompanying the transition to $^2E_{3/2}$ is B_5. It is attributed to excitation of $1\nu_7$, its energy value (0.151 eV) being very close to that of ν_7 in the electronic ground state of the neutral molecule (see Table I[27,28]). In support of this

TABLE II. Energy values (electron volts) and assignments of the vibrational structure of the HeI photoelectron bands corresponding to the ionization of the HOMO. The energy is given relative to the electronic origins B_1 and C_1.

		Assignment		
Band	Energy	State $^2E_{3/2}$	State $^2E_{1/2}$	Description
B_0	−0.068	$1\nu_{10}$		C–Br stretch
B_1	0	⋯		⋯
B_2	0.048	$1\nu_{10}$		C–Br stretch
B_3	0.090	$2\nu_{10}$		
B_4	0.116	$1\nu_9$		C–C stretch
B_5	0.151	$1\nu_7$		CH_2 wag
B_6	0.199	$1\nu_7+1\nu_{10}$		⋯
C_0	−0.065		$1\nu_{10}$	C–Br stretch
C_1	0		⋯	⋯
C_2	0.055		$1\nu_{10}$	C–Br stretch
B_7	0.379	$1\nu_{12}$		CH_2 antisymmetric stretch
B_8	0.426/0.118	$1\nu_{12}+1\nu_{10}$	$1\nu_9$	⋯/C–C stretch
C_3	0.153		$1\nu_7$	CH_2 wag
C_4	0.192		$1\nu_7+1\nu_{10}$	⋯
B_9	0.526	$1\nu_7+1\nu_{12}$		⋯
C_5	0.273		$1\nu_7+1\nu_9$	⋯
C_6	0.302		$2\nu_7$	⋯
C_7	0.368		$1\nu_2$	CH_2 symmetric stretch

assignation, the same vibrational mode has been observed for bromobutane (energy 0.149 eV) by both photoionization[12] and PES.[34] The shoulder on the low energy side of B_5 [Fig. 1(a)] is partly resolved into two features, B_3 and B_4, after deconvolution [Fig. 1(b)]. The more intense of them, B_4, is assigned to excitation of $1\nu_9$ (energy 0.116 eV). Peak B_7, partly resolved from C_1 in the raw spectrum and more visible in the deconvoluted one, lies at 0.379 eV from B_1. We assign it to excitation of $1\nu_{12}$, the energy value being consistent with that of ν_{12} in the electronic ground state (Tables II and III[27,28]). The low intensity features B_3, B_6, B_8, and B_9, located at 0.090, 0.199, 0.426, and 0.526 eV, respectively, from the electronic origin cannot, from these frequencies, be reasonably assigned to fundamental vibrational modes. Accordingly, B_3 is taken as the harmonic $2\nu_{10}$, and B_6, B_8, and B_9 as the combinations $1\nu_7+1\nu_{10}$, $1\nu_{12}+1\nu_{10}$, and $1\nu_7+1\nu_{12}$, respectively.

TABLE III. Vibrational energies (in electron volts) of C_2H_5Br. The energies values of the electronic ground state of the neutral molecule are taken from Refs. 27 and 28.

Species	C_2H_5Br	C_2H_5Br		$C_2H_5Br^+$	
Electronic[a] configuration	$(2e)^4$	$(2e)^3(6sa_1)^1$		$(2e)^3$	
Final state[a]	$\tilde{X}\,^1A_1$	$E(1)$	$E(3)$	$^2E_{3/2}$	$^2E_{1/2}$
ν_{10}[b]	⋯	⋯	⋯	0.068	0.065
ν_{10}	0.071	0.071	⋯	0.048	0.055
ν_9	0.120	0.114	⋯	0.116	0.118
ν_7	0.156	0.145	0.142	0.151	0.153
ν_2	0.364	⋯	⋯	⋯	0.368
ν_{12}	0.375	⋯	⋯	0.379	⋯
$2\nu_{10}$	⋯	⋯	⋯	0.090	⋯
$2\nu_7$	⋯	⋯	0.303	⋯	0.302
$\nu_7+\nu_{10}$	⋯	⋯	⋯	0.199	0.192
$\nu_7+\nu_9$	⋯	⋯	⋯	⋯	0.273
$\nu_{12}+\nu_{10}$	⋯	⋯	⋯	0.426	⋯
$\nu_2+\nu_7$	⋯	⋯	0.503	⋯	⋯
$\nu_{12}+\nu_7$	⋯	⋯	⋯	0.526	⋯

[a]The configuration and the final states are in the notation of the C_{3v} approximation.

[b]Energy value for ν_{10} in hot bands.

2. The $^2E_{1/2}$ state and its vibrational progression

The vibrational structure accompanying the transition to $^2E_{1/2}$ is similar to that of the $^2E_{3/2}$ state. Feature C_0, appearing as a weak shoulder on the low energy side of C_1 but better resolved in the deconvoluted spectrum [Fig. 1(b)], is located 0.065 eV below the origin (C_1) and is assigned to the $1\nu_{10}$ hot band. Feature C_2, appearing as a shoulder on B_7 in the deconvoluted spectrum [Fig. 1(b)], is attributed to excitation of $1\nu_{10}$ (0.055 eV). The most intense vibrational peak, C_3, is due to excitation of $1\nu_7$ (0.153 eV). The very weak band C_7 located at 0.368 eV (see Tables II and III[27,28]) from the electronic origin is assigned to $1\nu_2$, this value being close to that of $1\nu_2$ in the neutral molecular ground state. Consistent with this assignment, the relative intensity is similar to that of the corresponding band of methyl bromide.[33] In the $^2E_{3/2}$ state of $C_2H_5Br^+$, excitation of $1\nu_{12}$ is responsible for a band located at 0.379 eV from the electronic origin and with a relatively large intensity. The low intensity feature B_8, already assigned to the combination $1\nu_{12}+1\nu_{10}$ associated with the $^2E_{3/2}$ state is located at 0.118 eV from C_1, and thus may also hold a contribution from excitation of the normal vibrational mode $1\nu_9$ in $^2E_{1/2}$, this being weakly excited in the $^2E_{3/2}$ state. Features C_4, C_5, and C_6 are located at 0.192, 0.273, and 0.301 eV, respectively, from the electronic origin; as none of the fundamental frequencies of the neutral molecule approach these values, C_4 and C_5 are taken as the combinations $1\nu_7+1\nu_{10}$ and $1\nu_7+1\nu_9$, respectively, and C_6 the harmonic $2\nu_7$ (Tables II and III[27,28]).

B. The electronic excitation spectrum

The total photoabsorption spectrum is presented in Fig. 2. It consists of a broadband of low cross section between 5 and 6.7 eV and of sharp peaks of much larger cross section from 6.7 to 10.1 eV. These sharp features are superimposed on continuous absorptions with maxima in intensity around 7.4 and 8.3 eV. The form of the VUV spectrum is confirmed by the electron energy loss spectrum (Fig. 3). However, the latter extends up to 14.1 eV and shows at least one additional broadband with maximum intensity at 11.8 eV. In the 10.0–11.8 eV region, the EEL spectrum is similar to a photoabsorption spectrum published previously,[12] for spectral features, overall shape, and absolute cross sections. The intensity of the photoabsorption features between 8.83 and 10.1 eV (Figs. 2 and 3) is affected by degradation in the transmission of the LiF windows. Figure 4 gives enlargements of two regions: (a) from 6.8 to 8.6 eV and (b) from 8.6 to 10.1 eV.

1. The 5.0–6.7 eV region

The lowest energy electronic transition is responsible for the broad, weak absorption centered at 6.1 eV, and labeled the *A* band. It involves the promotion of an electron from the

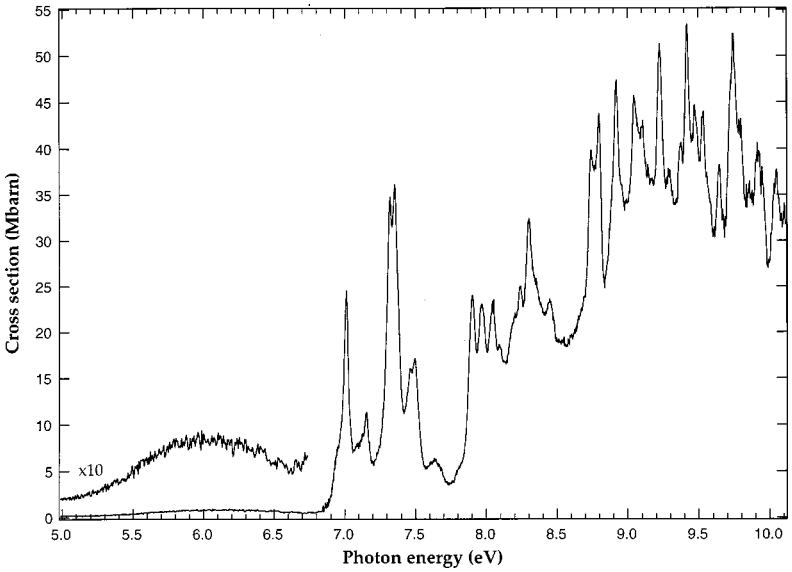

FIG. 2. High resolution photoabsorption spectrum of C_2H_5Br from 5.0 to 10.1 eV.

bromine $4p$ lone pair to the σ^* orbital which is antibonding along the C–Br bond.[1,10,13] In the alkyl halides, the transition $n \rightarrow \sigma^*$ is expected to lead to three excited states: $^3Q_1$, $^3Q_0$, and $^1Q_1$.[10] These states have been observed in ethyl and methyl iodide.[35–37] In the methyl bromide molecule, only the excitation to $^1Q_1$ has been reported[35] with a significant intensity, that of $^3Q_0$ being strongly reduced. The spin–orbit coupling being weaker in bromine than in iodine, a reduction of the intensity of the singlet–triplet transition is expected compared to that of the singlet–singlet transition.[35]

2. The 6.7–10.1 eV region

This region, displayed in Figs. 4(a) and 4(b) with peak labels, consists of several relatively intense absorption features, most of which are interpreted as members of Rydberg series converging to the two ionization limits $^2E_{3/2}$ and $^2E_{1/2}$. Their classification in terms of Rydberg series is made using the formula: $E_n = E_i - R/(n-\delta)^2$, where E_n is the peak energy position, E_i is the ionization energy (see the PES data, Sec. III A), R is the Rydberg constant, and δ is the quantum defect. For a bromine-containing molecule, the δ values ranges[1,15,38] are: $2.8 < \delta < 3.1$ for $ns(\lambda)$, $2.5 < \delta < 2.7$ for $np(\lambda)$, and $1.0 < \delta < 1.2$ for $nd(\lambda)$. The Rydberg series will be separated into a_1, e and e, corresponding to σ, π, and δ in the pseudoatomic model,[39] respectively. The energy values of the photoabsorption features, the excitation energies reported previously, and the assignment are given in Tables III and IV.

a. The nsa_1 Rydberg series. The region between 6.8 and 7.87 eV [Fig. 4(a)] shows two intense absorption bands, traditionally called *B* and *C*, accompanied by less intense features. It has been interpreted as arising from the transition $4p(e) \rightarrow 5s(a_1)$[14,15] which leads to states $E(2)$ and $E(1)$ for the $^2E_{3/2}$ ionic limit and to states A_1 and $E(3)$ for the $^2E_{1/2}$ limit.

The 0–0 transitions to the optically allowed states $E(1)$ and $E(3)$ are attributed to peaks 2 and 7, respectively, as

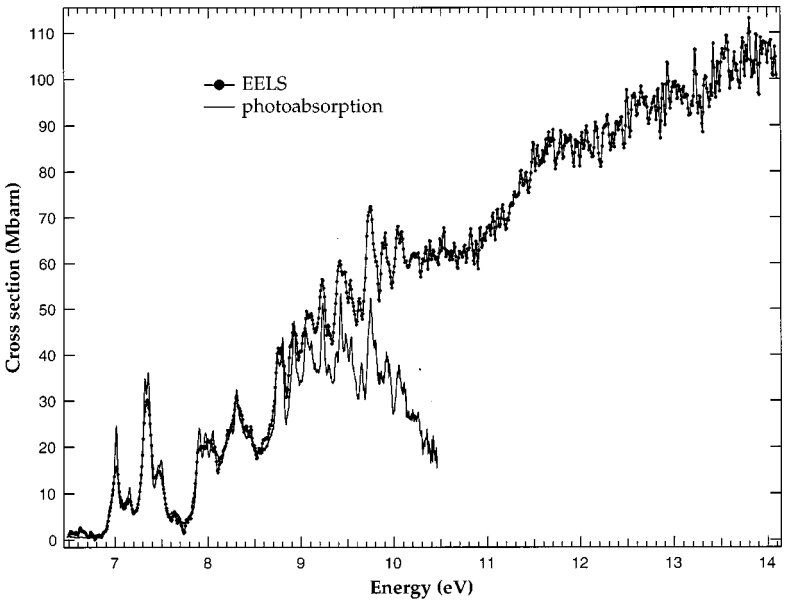

FIG. 3. Comparison of the C_2H_5Br photoabsorption spectrum with the EEL spectrum. For this, the EELS data were normalized to the photoabsorption cross-section value at 6.8 eV.

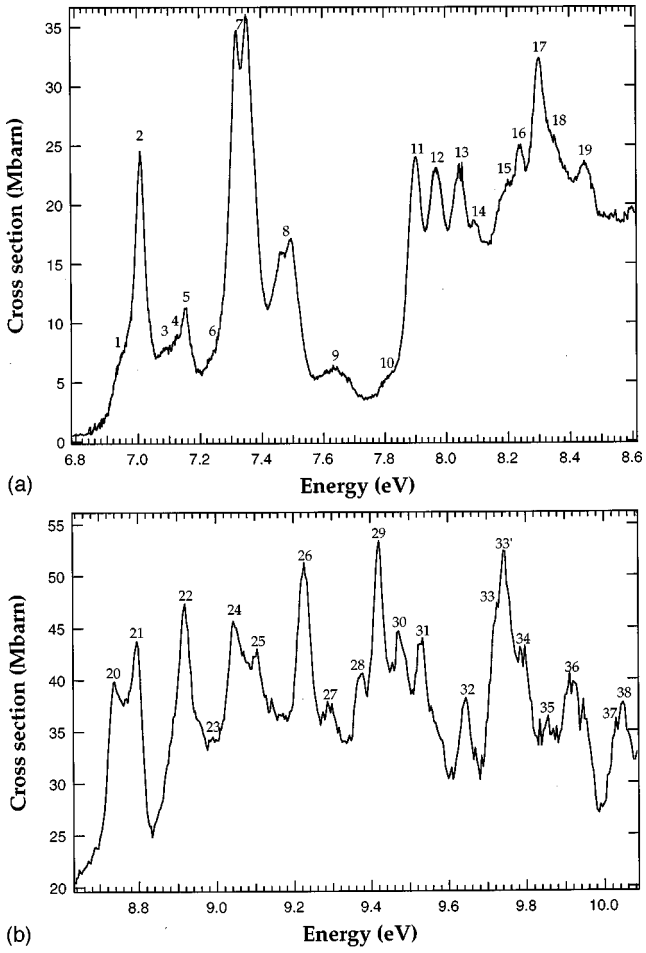

FIG. 4. High resolution photoabsorption spectra of the Rydberg states region of bromoethane: (a) 6.8–8.6 eV, (b) 8.6–10.1 eV.

they are the most intense bands in the spectral region and are separated by 0.32 eV, a value close to the spin–orbit splitting of the ion. The less intense feature 1, appearing as a shoulder on the low energy side of peak 2 and located at 6.964 eV, is assigned to transition to $E(2)$. Excitation of the state A_1 is suggested as being responsible for the weak band 6, located at 7.251 eV, its low intensity being compatible with the forbiddeness of the transition. The electronic origin assignments are in agreement with the literature data.[14,15]

The vibrational structure built on state $E(1)$ (peak 2) is interpreted by comparison with the PES spectrum. Accordingly, the weak features 3 and 4, partly resolved from peak 5 [Fig. 4(a)], and located at 0.071 and 0.114 eV from the origin are taken as excitation of $1\nu_{10}$ and $1\nu_9$, respectively. Band 5, 0.145 eV from the electronic origin, is assigned to the excitation of $1\nu_7$ (Table III). For $E(3)$, the presence of a doubling of the absorption bands 7 and 8 [Fig. 3(a)] has been ascribed to vibronic coupling between Rydberg states of the same configuration, i.e., $E(1)$ and $E(3)$, mediated by totally symmetric vibrational modes such as ν_1, ν_2, and ν_3.[15] Then, the vibrational progressions are determined from the barycenter of the split absorption peak 7 of the 0–0 transition, as has been done previously.[15] Feature 8 is due to excitation of $1\nu_7$ with an energy of 0.142 eV. The broadband 9 (7.64 eV) is supposed to contain excitation of the harmonic $2\nu_7$, in agreement with the PES spectrum (see Table III[27,28]) and previous work.[15] The weak feature 10, partly resolved from band 11 and located at 7.84 eV, is assigned to $1\nu_7+1\nu_2$.

Absorption bands 22 and 26, located at 8.918 and 9.226 eV [see Fig. 4(b)], are separated by 0.308 eV, which is close to the molecular spin–orbit coupling. They are assigned to the $n=6$ members of the $nsa_{1(3/2)}$ and $nsa_{1(1/2)}$ Rydberg series. The δ values of 2.86 and 2.87 are consistent with those reported previously.[15] The weak band 23 located at 0.067 eV from peak 22 may be due to the excitation of $1\nu_{10}$. Features 27 and 28 separated from peak 26 by 0.069 and 0.144 eV are suggested to be due to $1\nu_{10}$ and $1\nu_7$, respectively. At higher energy, features 30 and 34, located at 9.475 and 9.797 eV, are assigned to the $7sa_1$ members of the series converging to the two ionic limits, given the quantum defect of 2.94 and energy separation, 0.311 eV, which is close to the spin–orbit splitting of the ion. Feature 34 may also hold a contribution from the $8sa_1$ Rydberg state of the $^2E_{3/2}$ series, with a quantum defect of 2.80 (Table IV). The member $8sa_1(1/2)$ falls outside the spectral range of this work.

b. The np(λ) Rydberg series. The region between 7.9 and 8.6 eV [see Figs. 4(a) and 4(b)] has been attributed to excitation of the $5p(\lambda)$ series. The photoabsorption peaks 11 and 16 as well as 12 and 17 are separated by energy values close to the spin–orbit splitting of the ion. Therefore, it is proposed that features 11 at 7.902 eV and 16 at 8.24 eV are due to excitation of $5pa_1(3/2)$ and $5pa_1(1/2)$, respectively, the quantum defect of 2.58 and 2.57 being consistent with promotion to a $5p(\lambda)$ Rydberg orbital. Features 12 at 7.970 eV and 17 at 8.302 eV are assigned to $5pe_1(3/2)$ and $5pe_1(1/2)$, with δ of 2.62 and 2.60, respectively, in agreement with literature.[15] Peak 13 and the weak feature 18, partly resolved from photoabsorption band 17 are located at 0.142 and 0.140 eV from the $5pa_1(3/2)$ and $5pa_1(1/2)$ states, respectively, consistent with excitation of one quantum of the vibrational mode ν_7. For the two $5pe$ members, excitation of $1\nu_7$ is found at 0.142 eV (peak 14) and 0.143 eV (19), respectively, from the origins.

The $n=6$ terms of the two npa_1 series are assigned to the features 25 and 29 which are located at 9.101 and 9.42 eV, respectively, as their separation is close to the spin–orbit splitting of the molecular ion and the δ values are 2.63 and 2.62. Features 25 and 29, both broad, may be composites and contain contributions from the $nd(\lambda)$ series (see the following and Table IV). Transitions to $7pa_1(3/2)$ and $7pa_1(1/2)$ are assumed to be responsible for the spectral features 32 and 36, given the quantum defects 2.45 and 2.47 and by their energy separation of 0.304 eV, close to the molecular spin–orbit splitting.

c. The nd(λ) Rydberg series. In agreement with previous work[15] peaks 20 and 24 [Fig. 4(b)], separated by 0.308 eV, are due to the $4da_1$ members of the two series, their energy separation being close to the molecular ion spin–orbit splitting. The quantum defect is 1.05, which is consistent with $4d(\lambda)$ excitation. Features 21 and 25, which are separated by 0.306 eV, are ascribed to excitation of the $n=4$ terms of an nde series with $\delta=1.00$. Peaks 29 and 33 are assigned to transitions to $5da_1(3/2)$ and $5da_1(1/2)$, respec-

TABLE IV. Energy values (electron volts) of the absorption bands and assignments for the Rydberg states.

Components 3/2				Components 1/2				
Peak	This work	Previous work	δ	Peak	This work	Previous work	δ	Attributions
2	7.008	7.005[a,b] 7.007[c]	2.97	7	7.32	7.228[a] 7.353[b] 7.350[c]	2.97	$5sa1$
22	8.918	8.202[c]	2.86	26	9.226	9.208[c]	2.87	$6sa1$
30	9.475	⋯	2.94	34	9.797	⋯	2.94	$7sa1$
34	9.797	⋯	2.80	⋯	⋯	⋯	⋯	$8sa1$
11	7.902	7.896[a] 7.894[c]	2.62	16	8.24	8.228[c]	2.60	$5pa1$
12	7.970		2.58	17	8.302	⋯	2.57	$5pe$
25	9.101	⋯	2.63	29	9.420	⋯	2.62	$6pa1$
32	9.643	⋯	2.45	36	9.947	⋯	2.47	$7pa1$
20	8.736	8.719[c]	1.05	24	9.044	9.028[c]	1.05	$4da1$
21	8.795	⋯	1.00	25	9.101	⋯	1.00	$4de$
29	9.420	⋯	1.07	33	9.727	⋯	1.08	$5da1$
33′	9.743	⋯	1.06	38	10.046	⋯	1.09	$6da1$
37	9.915	⋯	1.06	⋯	⋯	⋯	⋯	$7da1$

[a]Reference 1.
[b]Reference 14.
[c]Reference 15.

tively. Again, their spacing of 0.307 eV is close to the molecular ion spin–orbit splitting and the quantum defects of 1.07 and 1.08, respectively, are close to those of $n=4$ of the nda_1 series (Table IV). Peak 33, being intense and rather broad, probably holds a contribution from excitation of $6da_1(3/2)$, labeled 33′, with a quantum defect of 1.06. The member $6da_1$ of the series converging to the other ionic limit is found at 10.046 eV [feature 38, Fig. 4(b)]. The energy spacing (0.303 eV) and the δ value support this assignment. The weak feature 37, on the low energy side of 38, located at 9.915 eV, could be responsible for the transition to $n=7$ of the $nda_1(3/2)$ series ($\delta=1.06$). Excitation of the $7da_1(1/2)$ state falls outside the energy range of the present work.

C. Differential and optical oscillator strengths

The electronic excitation spectra of ethyl bromide measured by photoabsorption and by EELS are displayed in Fig. 3 for the 6.5–14.004 eV region. Comparison of the optical absorption cross-sections values with those of the EELS data shows the optical measurements to be free of line saturation effects. The EEL spectrum gives access to the oscillator strength values up to 14.004 eV, that is into a region which is inaccessible in our photoabsorption experiment.

For the lowest energy valence absorption band, the cross-section value reported in Fig. 1 agrees with that deduced from the extinction coefficients.[9,11]

For the Rydberg state region, as shown in Fig. 3, the photoabsorption spectrum is similar to the normalized EEL spectrum. Differences arise only from different energy resolution between the two experiments. Table V gives the optical oscillator strength values obtained from EELS and optical UV photoabsorption. The electron impact data and the photoabsorption data match until 8.83 eV. This confirms that the photoabsorption cross-section values are free of line saturation effects, and are believed to be accurate up to 8.83 eV. From 8.83 to 10.1 eV (the limit of the present optical spectrum), the two values diverge but we know this to be due to degradation in the transmission of the LiF windows. The EEL data are therefore preferred from 8.83 to 14.004 eV as absolute cross-section measurements. They match well with the photoabsorption cross-section values reported previously in the 10–to 11.8 eV range[12] (limit of the cited experiment), enhancing confidence in the present EELS measurements.

IV. CONCLUSIONS

The electronic spectroscopy of ethyl bromide has been studied in the 5.056–14.004 eV range by both high resolution photoabsorption and electron impact. Tentative assignments in the spectral region corresponding to electronically excited states involving electron transitions from the highest occupied molecular orbital into the $5s$ Rydberg orbital have been made by comparison with a new high resolution photoelectron spectrum related to the HOMO. Our attribution of the $5sa_1$ and $5pa_1$ members of the two series is in agree-

TABLE V. Optical oscillator strength for ethyl bromide.

Energy region (eV)	Photoabsorption	EELS
5.056–6.698	0.009	⋯
6.7605–7.7472	0.090	0.084
7.7495–8.1337	0.054	0.053
8.1337–8.5624	0.088	0.092
8.5624–8.8341	0.069	0.078
8.8341–10.127	0.446	0.630
10.132–10.612	⋯	0.271
10.612–12.02	⋯	0.962
12.02–14.004	⋯	1.74

ment with the literature.[1,14,15] We also confirm the previous identification of the $6sa_1$ and $4da_1$ series[15] and report new members of the nsa_1, npa_1, and nda_1 Rydberg series. The npe and nde series are observed for the first time.

Oscillator strength values have also been measured by EELS and VUV photoabsorption in the region of 6.5–14.004 eV. These data could be used as standards for any future photoabsorption experiment.

ACKNOWLEDGMENTS

This research has been supported by the Patrimoine of the University of Liège, the Fonds National de la Recherche Scientifique, and the Fond de la Recherche Fondamentale Collective. It has been funded in part by the EPSRC and CLRC of the United Kingdom. M.J.H.F. wishes to acknowledge the Fonds National de la Recherche Scientifique for position. J.M.G. and N.C.J. recognize the provision of EPSRC postgraduate studentships. N.J.M. recognizes the support of the Royal Society. M.J.H.F., N.J.M., J.M.G., and N.C.J. are grateful to NATO for a collaborative research grant. M.J.H.F. benefits of an INTAS contract. The technical assistance of Jacques Heinesch is highly acknowledged.

[1] M. B. Robin, *Higher Excited States of Polyatomic Molecules* (Academic, New York, 1974), Vol. I.
[2] K. Suto, Y. Sato, C. L. Reed, V. Skorokhodov, Y. Matsumi, and M. Kawasaki, J. Phys. Chem. **101**, 1222 (1997).
[3] E. Lehrer, D. Wagenbach, and U. Platt, Tellus **49**, 486 (1997).
[4] C. Chiorbolo, R. Piazza, V. Carassiti, L. Passerini, A. Pino, M.-L. Tosato, and D. Riganelli, Gazz. Chim. Ital. **126**, 685 (1996).
[5] M. Kosugi and N. Harada, European Patent No. 0 374 036 (12/10/1994).
[6] P. Brewer, S. Hale, and R. M. Osgood, Jr., Appl. Phys. Lett. **45**, 477 (1985).
[7] W. C. Price, J. Chem. Phys. **4**, 547 (1936).
[8] G. Scheibe, F. Povenz, and C. Lindstrom, Z. Phys. Chem. Abt. B **20**, 283 (1933).
[9] D. Porret and C. F. Goodeve, Proc. R. Soc. London, Ser. A **165**, 31 (1938).
[10] R. S. Mulliken, Phys. Rev. **47**, 413 (1935); J. Chem. Phys. **8**, 382 (1940).
[11] N. Astoin, J. Garnier, and M. Cordier, J. Phys. **19**, 507 (1958).
[12] J. C. Person and P. P. Nicole, J. Chem. Phys. **55**, 3390 (1971).
[13] K. Kimura and S. Nagakura, Spectrochim. Acta. **17**, 166 (1961).
[14] N. L. Baker and B. R. Russel, J. Mol. Spectrosc. **69**, 221 (1978).
[15] W. S. Felps, J. D. Scott, G. L. Findley, and S. P. McGlynn, J. Chem. Phys. **74**, 4832 (1981).
[16] J. Delwiche, P. Natalis, J. Momigny, and J. E. Collin, J. Electron Spectrosc. Relat. Phenom. **1**, 219 (1972).
[17] F. Motte-Tollet, J. Delwiche, J. Heinesch, M.-J. Hubin-Franskin, J. M. Gingell, N. C. Jones, N. J. Mason, and G. Marston, Chem. Phys. Lett. **284**, 452 (1998).
[18] J. H. D. Eland, *Photoelectron Spectroscopy*, 2nd ed. (Butterworth, London, 1984).
[19] P. H. Van Cittert, Z. Phys. **69**, 298 (1931).
[20] J. D. Allen, Jr. and F. A. Grimm, Chem. Phys. Lett. **66**, 72 (1979).
[21] M. H. Palmer, I. C. Walker, M. F. Guest, and M. R. F. Siggel, Chem. Phys. **201**, 381 (1995).
[22] J. M. Gingell, N. J. Mason, H. Zhao, I. C. Walker, and M. R. F. Siggel, Chem. Phys. **220**, 191 (1997).
[23] M. Furlan, M.-J. Hubin-Franskin, J. Delwiche, D. Roy, and J. E. Collin, J. Chem. Phys. **82**, 1797 (1985).
[24] F. Motte-Tollet, M.-J. Hubin-Franskin, and J. E. Collin, J. Chem. Phys. **97**, 7314 (1992).
[25] F. Motte-Tollet, J. Heinesch, J. M. Gingell, and N. J. Mason, J. Chem. Phys. **106**, 5990 (1997).
[26] R. H. Huebner, R. J. Celotta, S. R. Mielczarek, and C. E. Kuyatt, J. Chem. Phys. **59**, 5434 (1973).
[27] R. Gaufès and M. Béjaud-Bianchi, Spectrochim. Acta A **27**, 2249 (1970).
[28] C. F. Wilcox, Jr. and S. H. Bauer, Spectrochim. Acta A **52**, 207 (1996).
[29] A. Giuliani *et al.*, J. Chem. Phys. **110**, 10307 (1999).
[30] J. A. Hashmall and E. Heilbronner, Angew. Chem. Int. Ed. Engl. **9**, 305 (1970).
[31] F. Brogli and E. Heilbronner, Helv. Chim Acta **54**, 1423 (1971).
[32] K. Kimura, S. Katsumata, Y. Achiba, H. Matsumoto, and S. Nagakura, Bull. Chem. Soc. Jpn. **46**, 373 (1973).
[33] L. Karlsson, R. Jadrny, L. Mattsson, F. T. Chan and K. Siegbahn, Phys. Scr. **16**, 25 (1977).
[34] I. Novak, L. Klasinc, B. Kovac, and J. P. Mc Glynn, J. Mol. Struct. **297**, 383 (1993).
[35] A. Gedanken and M. D. Rowe, Chem. Phys. Lett. **34**, 39 (1975).
[36] A. Gedanken, Chem. Phys. Lett. **137**, 462 (1987).
[37] A. Bouguerne, M. J. Hubin-Franskin, and M. Furlan, J. Phys. B **27**, 199 (1994).
[38] A. B. F. Duncan, *Rydberg Series in Atoms and Molecules* (Academic, New York, 1971).
[39] E. Lindholm, Ark. Fys. **10**, 125 (1969).